Environment-driven quenching of star formation:

Evidence from the ages of red-sequence galaxies in the Coma Custer

Russell J. Smith (University of Durham)

John Lucey (Durham), James Price (Bristol), Mike Hudson (Waterloo), Ron Marzke (San Francisco State), Steve Allanson (Waterloo), Terry Bridges (AAO), David Carter (Liverpool John Moores), Ann Hornschemeier (NASA/GSFC), Neal Miller (Johns Hopkins)

ABSTRACT We use spectroscopic age estimates, for a sample of 362 dwarf and giant red-sequence galaxies in Coma, to investigate the role of environment in driving the quenching star of formation. **Section I** shows that age is significantly correlated with cluster-centric radius, R_{proj}, in Coma. **Section II** uses simulation data to show that we should expect environmental history to be correlated with R_{proj}. **Section III** shows that simple quenching models based on the halo merger histories yield cluster-centric age gradients consistent with the observations.

I. Observed gradients of stellar population ages

Our analysis is based on high-S/N spectroscopy from MMT for faint galaxies (M*+2 to M*+4), complemented with identical re-analysis of SDSS spectra at the bright end (Price et al. 2011). The full sample of 362 galaxies covers most of the area within the virial radius, and spans a factor of a thousand in mass. With the extended azimuthal coverage and mass range, we improve significantly on the results presented in Smith et al. (2009). Stellar ages are derived from comparison of absorption line indices against simple stellar population (SSP) models from Schiavon (2007). The key observational results on cluster-centric age trends are:

(1) After controlling for galaxy mass, there is a significant residual trend of age with projected cluster-centric radius, with slope of 0.07±0.02 dex/Mpc for the sample as a whole (Fig. 1).

(2) Stronger radial trends (0.13±0.03 dex/Mpc) are observed for dwarf galaxies (Figs. 1, 2).

(3) The age dependence is not localised to the sub-cluster centred on NGC 4839 in the South-West of Coma. Rather, the core of the cluster is unlike any part of the outskirts (Fig. 3).

(4) All our results are insensitive to which proxy is adopted for galaxy mass (velocity dispersion, dynamical mass, luminosity, stellar mass).

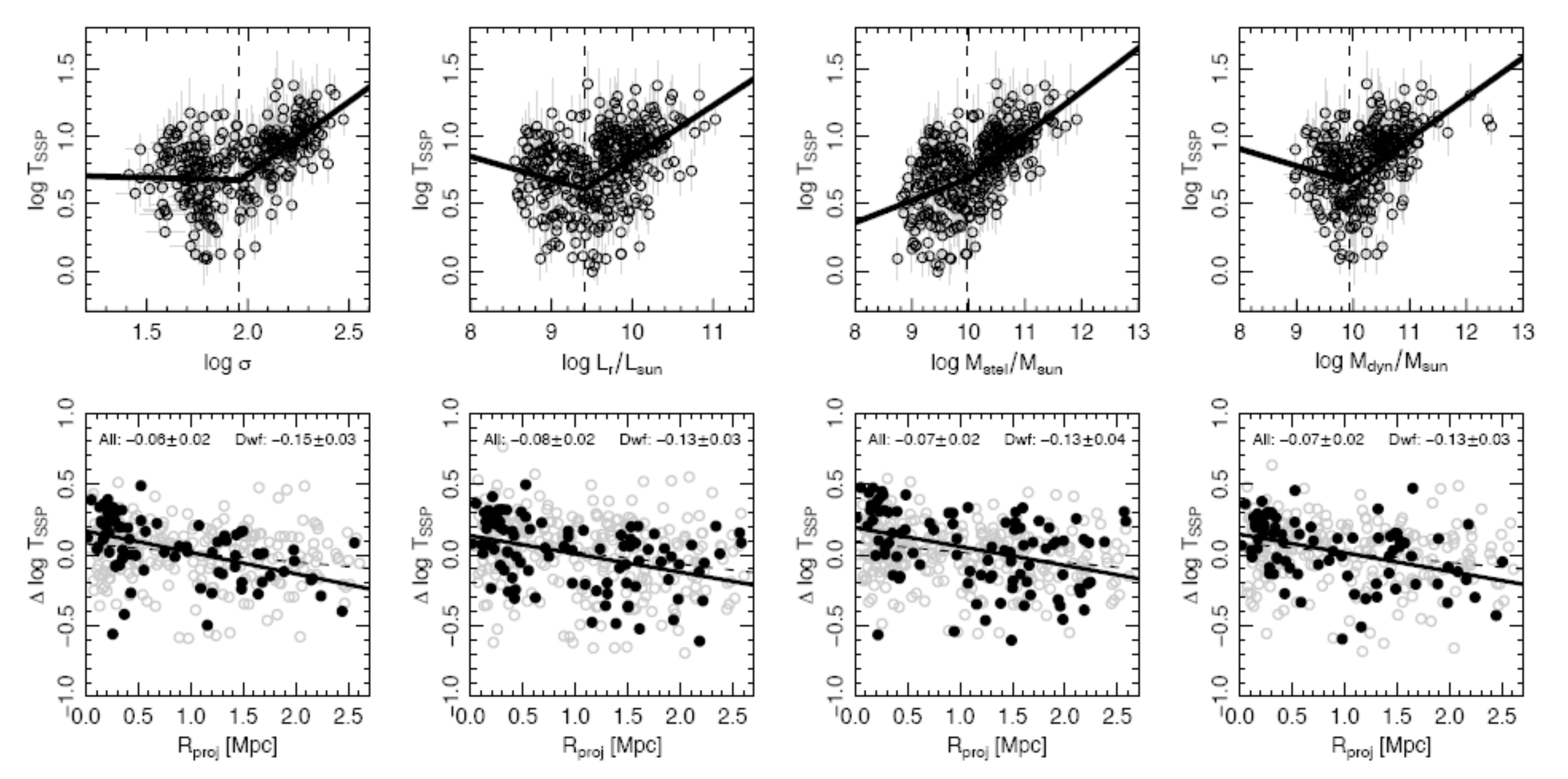

Figure 1: *Upper panels* The correlations of SSP-equivalent age versus galaxy "mass" for red-sequence galaxies in Coma from our combined MMT+SDSS sample. We show the relation for four different indicators of galaxy mass: velocity dispersion, luminosity, stellar mass and dynamical mass. Heavy lines show best-fit broken-stick regression model. *Lower panels* The residuals from the corresponding age-vs-mass relation, plotted against projected cluster-centric radius, R_{proj}. The dashed line is a linear fit the full sample; the solid line fits only the 25% lowest-mass galaxies in each panel, which are highlighted with black solid points. ***There is a significant anti-correlation of age with projected radius, which is stronger for the dwarf galaxies than for the whole sample.***

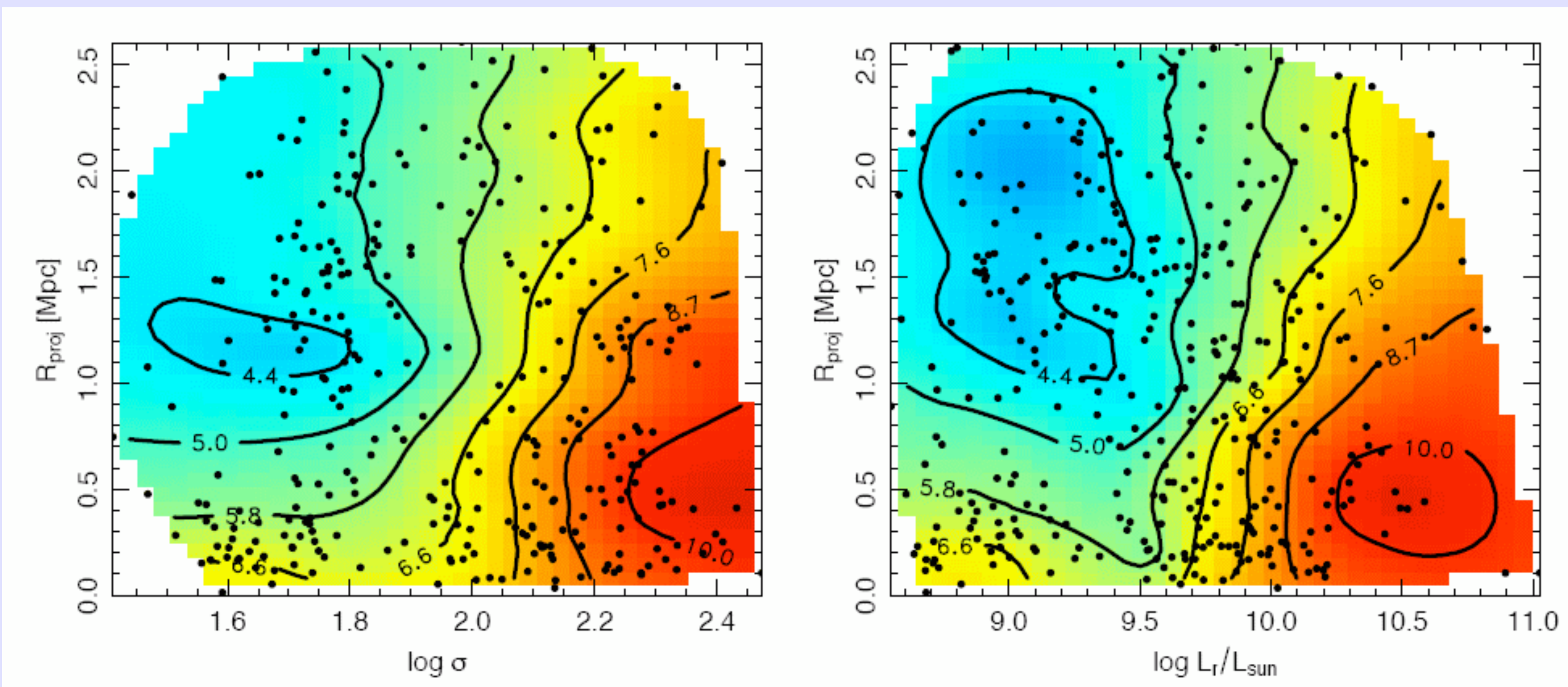

Figure 2: SSP-equivalent ages of red sequence galaxies in Coma, mapped as a function of "mass" (horizontal axis) and projected cluster-centric radius (vertical axis). The two panels show results using velocity dispersion and luminosity as proxies for mass (stellar mass and dynamical mass show similar behaviour). Black points show the location of the sample galaxies on the mass-radius plane. The colour map and contours (spaced logarithmically by 15%, with labels in Gyr) show the age surface. ***For giants, the contours are near vertical, indicating that their ages depend mostly on mass; for dwarfs, the contours bend almost horizontally: dwarf ages depend primarily on "environment".***

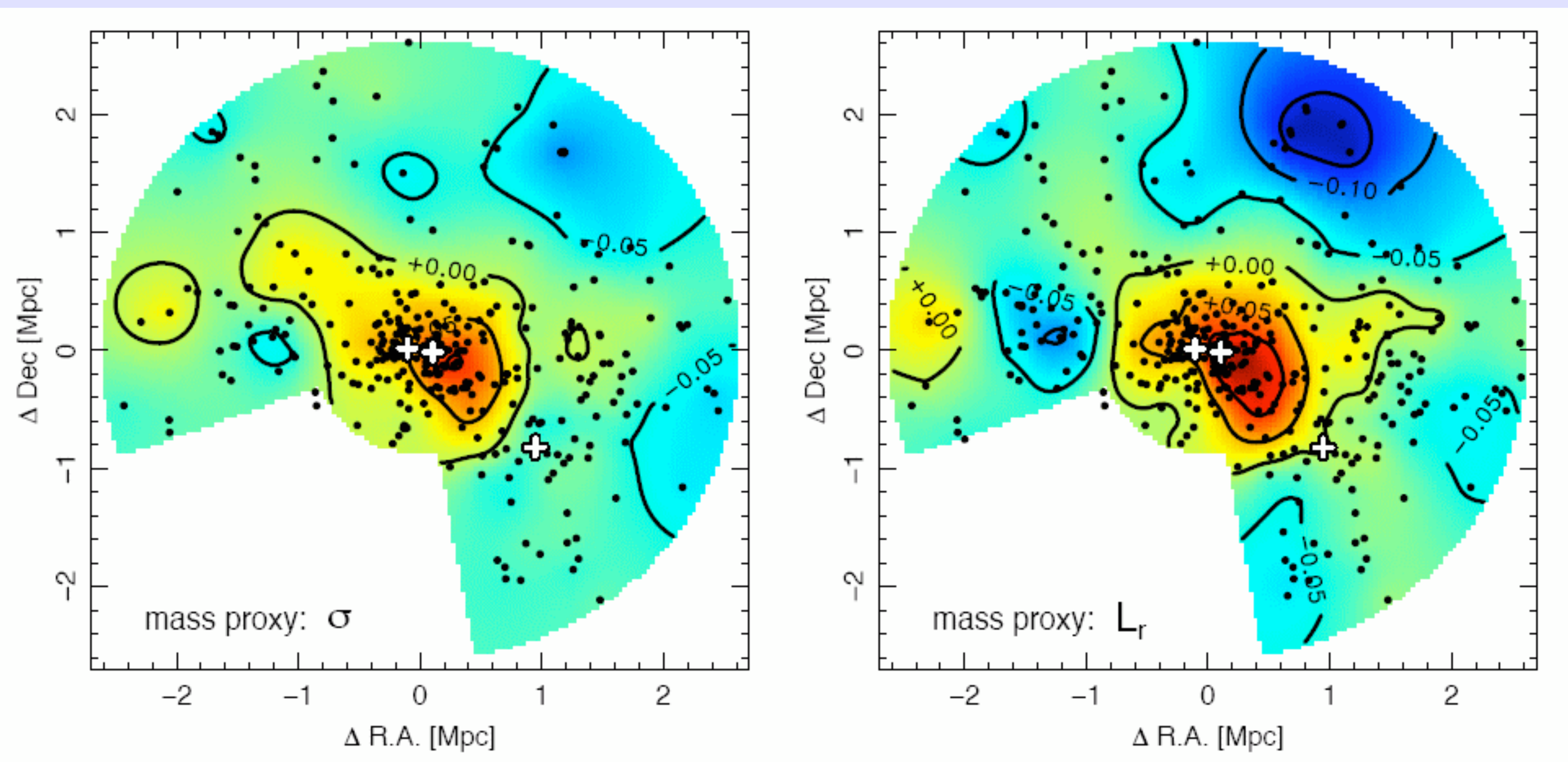

Figure 3: Residuals from the age-vs-"mass" relations, mapped as a function of projected location within the cluster. The panels show results when velocity dispersion and luminosity are used for the mass proxy. Results are qualitatively unchanged if stellar mass or dynamical mass is used. The colour map and contours (spaced at 0.05 dex) show the spatial variation in the average age residual. The locations of sample galaxies are indicated by the black points. Large white crosses show the positions of the three dominant galaxies NGC 4889, NGC 4874 and NGC 4839. ***The cluster-centric gradients are driven by older ages in the cluster core, not by a localized concentration of young galaxies in the South-West or elsewhere.***

II. Cluster-centric gradients in environmental history

To interpret the observed trends, we use the Millennium Simulation (Springel et al. 2005), and semi-analytic models of Font et al. (2008), to test whether the typical "environmental history" experienced by cluster galaxies depends on cluster-centric distance. We focus on the time when a galaxy became a member of a halo of mass $10^{12}\,M_{sun}$, $10^{13}\,M_{sun}$ or $10^{14}\,M_{sun}$, and the time when it last ceased to be a "central" galaxy within its halo.

The main result of this analysis (shown in Fig. 4) are:

(1) For all four definitions of the "environmental age", we find a clear gradient of ~0.2 dex/Mpc in the inner 1 Mpc, becoming flatter at larger radius.

(2) Galaxies in the outskirts at z=0 not only entered cluster-scale halos later than galaxies in the cluster core, but also joined group-scale halos later, and remained central galaxies of their own halo for longer.

(3) Thus even though many galaxies enter their eventual final cluster via accreted groups (McGee et al. 2009), group-scale environmental quenching processes should leave cluster-centric gradients in the final cluster.

(4) The environmental gradients do not depend on galaxy stellar mass, except in the case of the $10^{12}\,M_{sun}$ mass threshold, where dwarfs have steeper slope than giants.

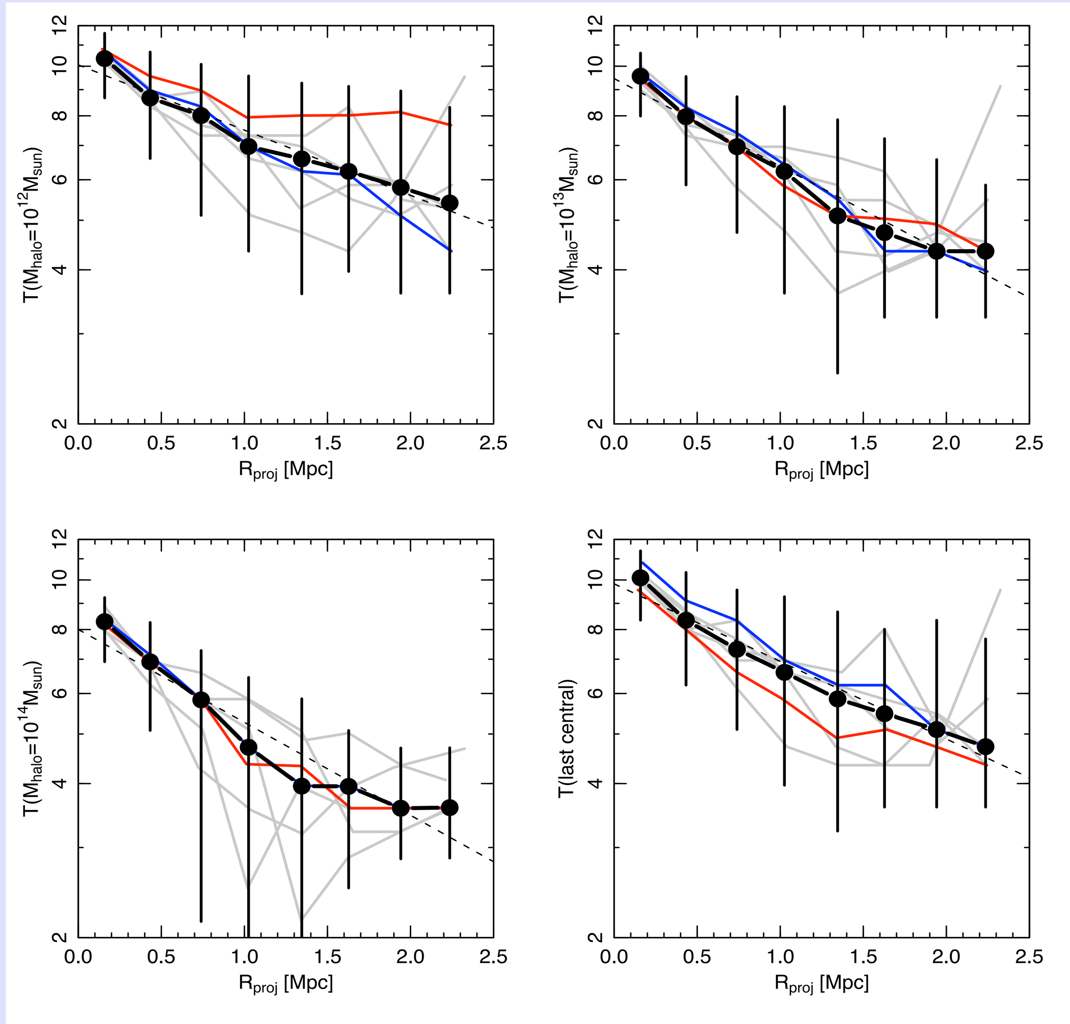

Figure 4: Correlation of "environmental ages" with projected cluster-centric distance, extracted from five $10^{15} M_{sun}$ clusters in the Millennium Simulation. Panels show time of different "events" in the accretion history. Black points are averages within bins; "error bars" show interquartile range. The grey profiles show the five individual halos and red and blue lines isolate the trends for the highest and lowest galaxy stellar masses. ***The accretion of cluster members into halos above a given threshold mass is correlated with projected location in the cluster at z=0, even for group-scale thresholds.***

III. Quenching models

Finally, we connect the environmental history to the observed stellar population ages by assuming that the environmental events explored above are associated with the quenching of star formation in galaxies. (The star-formation histories assigned by the semi-analytic model is ignored). We test different star-formation histories (abrupt quenching, quenching plus exponential decline, quenching plus final burst) to translate quenching time T_Q into measurable SSP-equivalent age T_{SSP} for comparison to the observed gradients (Tables 1, 2).

sample	Gradient in ΔT_{SSP} using mass proxy σ	M_{dyn}	L_r	M_{stel}	median gradient
All	-0.06 ± 0.02	-0.07 ± 0.02	-0.08 ± 0.02	-0.07 ± 0.02	-0.07
All inside 1 Mpc	-0.07 ± 0.06	-0.08 ± 0.06	-0.11 ± 0.07	-0.12 ± 0.06	-0.10
All excluding SW	-0.07 ± 0.02	-0.07 ± 0.02	-0.09 ± 0.02	-0.08 ± 0.02	-0.07
All in core and SW	-0.07 ± 0.03	-0.07 ± 0.03	-0.07 ± 0.03	-0.07 ± 0.02	-0.07
Dwarfs (25% lowest mass)	-0.15 ± 0.03	-0.13 ± 0.03	-0.13 ± 0.03	-0.13 ± 0.04	-0.13
Dwarfs inside 1 Mpc	-0.24 ± 0.11	-0.17 ± 0.11	-0.22 ± 0.12	-0.20 ± 0.15	-0.21
Dwarfs excluding SW	-0.14 ± 0.03	-0.10 ± 0.04	-0.13 ± 0.03	-0.12 ± 0.04	-0.13
Dwarfs in core and SW	-0.24 ± 0.05	-0.22 ± 0.05	-0.16 ± 0.05	-0.14 ± 0.06	-0.19

Table 1: The observed cluster-centric gradients of SSP-equivalent stellar age (after removing mass trend), for the full Coma sample, and for various subsets. Gradients are in units of dex / Mpc.

Table 2: Gradients in T_{SSP} predicted from maximally-efficient environmental quenching models. For example the first line assumes all galaxies are quenched when they become members of $10^{14}\,M_{sun}$ halos. In "burst/strangulation" models the predicted SSP age is equal to the quenching time. In "stripping" models, it is older, mimicking the effect of abruptly truncated SFH.

environmental quantity	— burst/strangulation — $R_{proj} < 1$ Mpc	$R_{proj} < 2.5$ Mpc	— stripping — $R_{proj} < 1$ Mpc	$R_{proj} < 2.5$ Mpc
$T(M_{halo} > 10^{14}\,M_\odot)$	-0.28 ± 0.19	-0.18 ± 0.05	-0.12 ± 0.07	-0.10 ± 0.03
$T(M_{halo} > 10^{13}\,M_\odot)$	-0.21 ± 0.09	-0.17 ± 0.05	-0.10 ± 0.05	-0.09 ± 0.03
$T(M_{halo} > 10^{12}\,M_\odot)$	-0.19 ± 0.09	-0.13 ± 0.05	-0.08 ± 0.05	-0.07 ± 0.02
T_{cent}	-0.21 ± 0.10	-0.15 ± 0.05	-0.09 ± 0.05	-0.08 ± 0.02
T_{sat}	-0.24 ± 0.09	-0.15 ± 0.06	-0.11 ± 0.05	-0.08 ± 0.03

The results of these experiments are:

(1) To first order the predicted gradients in T_{SSP} are 0.1-0.2 dex/Mpc, i.e. very comparable to the observed age trends.

(2) The predicted trends are not very sensitive to the definition adopted for environmental age: this test cannot discriminate the halo mass threshold responsible for quenching.

(3) Models with *abrupt* quenching (mimicking rapid "stripping" of cold gas from infalling galaxies) yield flatter slopes that those with exponentially-declining SFH after quenching (representing "strangulation"). This difference arises from the T_Q-to-T_{SSP} translation.

(4) The "stripping" models predict gradients too shallow to account for the observed trend in the dwarfs. The "strangulation" (and the quench+burst) models match the dwarf trends but are too steep for the sample as a whole.

IV. Conclusions

(1) Significant cluster-centric trends in the SSP-equivalent ages of red-sequence galaxies are observed in the Coma cluster.

(2) The observed age trends for dwarfs can be reproduced by models with environmental quenching via "strangulation", if this acts with maximal efficiency, i.e. all dwarfs quenched by environment.

(3) The weaker radial trends seen for more massive galaxies probably imply "internal" processes, uncorrelated with environment, dilute the gradients for giants.

(4) The agreement between data and models is generic and does not favour a particular halo mass threshold as responsible for stripping.

REFERENCES: Font 2008 et al. MNRAS 389, 1619; McGee S. et al. 2009, MNRAS, 400, 937; Price J. et al. 2011, MNRAS, 411, 2558; Schiavon R. 2007, ApJS 171, 146; Smith R.J., et al. 2006, MNRAS, 369, 1419; Smith R.J. et al. 2009, MNRAS, 392, 1265; Springel V. et al, 2005, Nature, 435, 629